Aspergillus fumigatus Strain-Specific Conidia Lung Persistence Causes an Allergic Broncho-Pulmonary Aspergillosis-Like Disease Phenotype

Jane T. Jones,[a] Ko-Wei Liu,[a] Xi Wang,[a] Caitlin H. Kowalski,[a] Brandon S. Ross,[a] Kathleen A. M. Mills,[b,c] Joshua D. Kerkaert,[a] Tobias M. Hohl,[b,c] Lotus A. Lofgren,[d] Jason E. Stajich,[d] Joshua J. Obar,[a] Robert A. Cramer[a]

aGeisel School of Medicine, Department of Microbiology and Immunology, Dartmouth, Hanover, New Hampshire, USA
bInfectious Disease Service, Department of Medicine, Memorial Sloan Kettering Cancer Center, New York, New York, USA
cImmunology and Microbial Pathogenesis Graduate Program, Weill Cornell Graduate School, New York, New York, USA
dDepartment of Microbiology and Plant Pathology, University of California Riverside, Riverside, California, USA

ABSTRACT *Aspergillus fumigatus* is a filamentous fungus which can cause multiple diseases in humans. Allergic broncho-pulmonary aspergillosis (ABPA) is a disease diagnosed primarily in cystic fibrosis patients caused by a severe allergic response often to long-term *A. fumigatus* colonization in the lungs. Mice develop an allergic response to repeated inhalation of *A. fumigatus* spores; however, no strains have been identified that can survive long-term in the mouse lung and cause ABPA-like disease. We characterized *A. fumigatus* strain W72310, which was isolated from the expectorated sputum of an ABPA patient, by whole-genome sequencing and *in vitro* and *in vivo* viability assays in comparison to a common reference strain, CEA10. W72310 was resistant to leukocyte-mediated killing and persisted in the mouse lung longer than CEA10, a phenotype that correlated with greater resistance to oxidative stressors, hydrogen peroxide, and menadione, *in vitro*. In animals both sensitized and challenged with W72310, conidia, but not hyphae, were viable in the lungs for up to 21 days in association with eosinophilic airway inflammation, airway leakage, serum IgE, and mucus production. W72310-sensitized mice that were recall challenged with conidia had increased inflammation, Th1 and Th2 cytokines, and airway leakage compared to controls. Collectively, our studies demonstrate that a unique strain of *A. fumigatus* resistant to leukocyte killing can persist in the mouse lung in conidial form and elicit features of ABPA-like disease.

IMPORTANCE Allergic broncho-pulmonary aspergillosis (ABPA) patients often present with long-term colonization of *Aspergillus fumigatus*. Current understanding of ABPA pathogenesis has been complicated by a lack of long-term *in vivo* fungal persistence models. We have identified a clinical isolate of *A. fumigatus*, W72310, which persists in the murine lung and causes an ABPA-like disease phenotype. Surprisingly, while viable, W72310 showed little to no growth beyond the conidial stage in the lung. This indicates that it is possible that *A. fumigatus* can cause allergic disease in the lung without any significant hyphal growth. The identification of this strain of *A. fumigatus* can be used not only to better understand disease pathogenesis of ABPA and potential antifungal treatments but also to identify features of fungal strains that drive long-term fungal persistence in the lung. Consequently, these observations are a step toward helping resolve the long-standing question of when to utilize antifungal therapies in patients with ABPA and fungal allergic-type diseases.

KEYWORDS *Aspergillus fumigatus*, chronic infection, allergic broncho-pulmonary aspergillosis, oxidative stress, genomics, ABPA, strain heterogeneity

ndividuals with atopic asthma, chronic obstructive pulmonary disease (COPD), and particularly cystic fibrosis (CF) are susceptible to chronic fungal colonization and infections in the lung (1). For example, 30 to 80% of CF patients persistently test positive for growth of the filamentous fungus *Aspergillus fumigatus* in expectorated sputum (2–4), and this finding is associated with overall decreased lung function (5). These findings demonstrate that *A. fumigatus* colonization is a critical aspect of CF disease pathogenesis. A subset of these patients develops allergic broncho-pulmonary aspergillosis (ABPA), a particularly difficult disease to diagnose and treat. Individuals with CF and/or asthma are typically diagnosed with ABPA and exhibit a type 2 immune response that leads to the production of high levels of interleukin 4 (IL-4), airway eosinophilia, and increased total and *A. fumigatus*-specific IgE (6, 7). Recurrent ABPA exacerbations lead to the development of bronchiectasis, airway remodeling, and fibrosis as a long-term consequence of fungal colonization (8). Although treating ABPA patients with antifungal drugs can improve symptoms in some cases (9, 10), it is not known how or whether persistence of *A. fumigatus* in the lungs specifically contributes to ABPA disease pathogenesis.

Murine models of fungal persistence using agar beads containing *A. fumigatus* conidia successfully recapitulated long-term (21 to 28 days) colonization of fungal hyphae in the lung (11, 12); however, mice in this specific agar bead model do not develop the strong IgE/Th2 response observed in ABPA patients. Numerous other mouse models that seek to recapitulate human ABPA have been described, including utilizing *A. fumigatus* antigens (13) and repeated challenge with live conidia (14), though none of these models exhibited long-term persistence of *A. fumigatus* in the airways, a common and important feature of ABPA (5, 15, 16). Importantly, the extent of fungal growth in ABPA patients' airways is unclear, though hyphae have been identified in sputum and tissue in some patient samples (17, 18). Consequently, *in vivo* studies examining the fungal contribution to ABPA development, persistence, and disease progression are currently difficult to conduct. This is a critical question to address because it is expected to help inform when antifungal therapies may be effective in the context of ABPA.

The goal of the current study was to identify a strain of *A. fumigatus* that is capable of long-term persistence in the lung of immunocompetent mice. Using a clinical strain isolated from a sputum sample of an ABPA patient, viable *A. fumigatus* was recovered from the murine airways for up to 21 days. Animals with persistent fungal burden developed increased serum IgE, eosinophilia, airway damage, mucus production, and an increased immune response to reexposure to fungi, all common features of ABPA. Surprisingly, these symptoms developed despite little to no hyphal growth observed in the airways of animals with persistent fungal burden. Consequently, these data demonstrate that a fungal strain with resistance to leukocyte killing and relatively low virulence is capable of long-term persistence in the murine lung and initiating ABPA-like disease pathogenesis.

RESULTS

***Aspergillus fumigatus* clinical isolate W72310 is resistant to immune cell-mediated killing and persists in the murine lung.** Previous work from our laboratory found that a clinical isolate strain, W72310, had reduced virulence compared to the commonly studied reference strain CEA10 in mice with suppressed immune systems (19). Conidia from W72310 have also been reported to germinate more slowly under a variety of conditions (20) in comparison to other *A. fumigatus* strains. We hypothesized that a slow-growing, less virulent strain may evade immune clearance and allow establishment of long-term fungal persistence in murine airways. In order to test this hypothesis, we first compared W72310 and CEA10 persistence in the immunocompetent murine lung 7 days after one fungal intranasal inoculation. Grocott-Gomori methenamine silver (GMS) staining of fixed lungs revealed that fungal conidia were still present in W72310-exposed lungs 7 days postinoculation; however, no observable conidia were found in CEA10-challenged animals (Fig. 1A). While swollen conidia could be
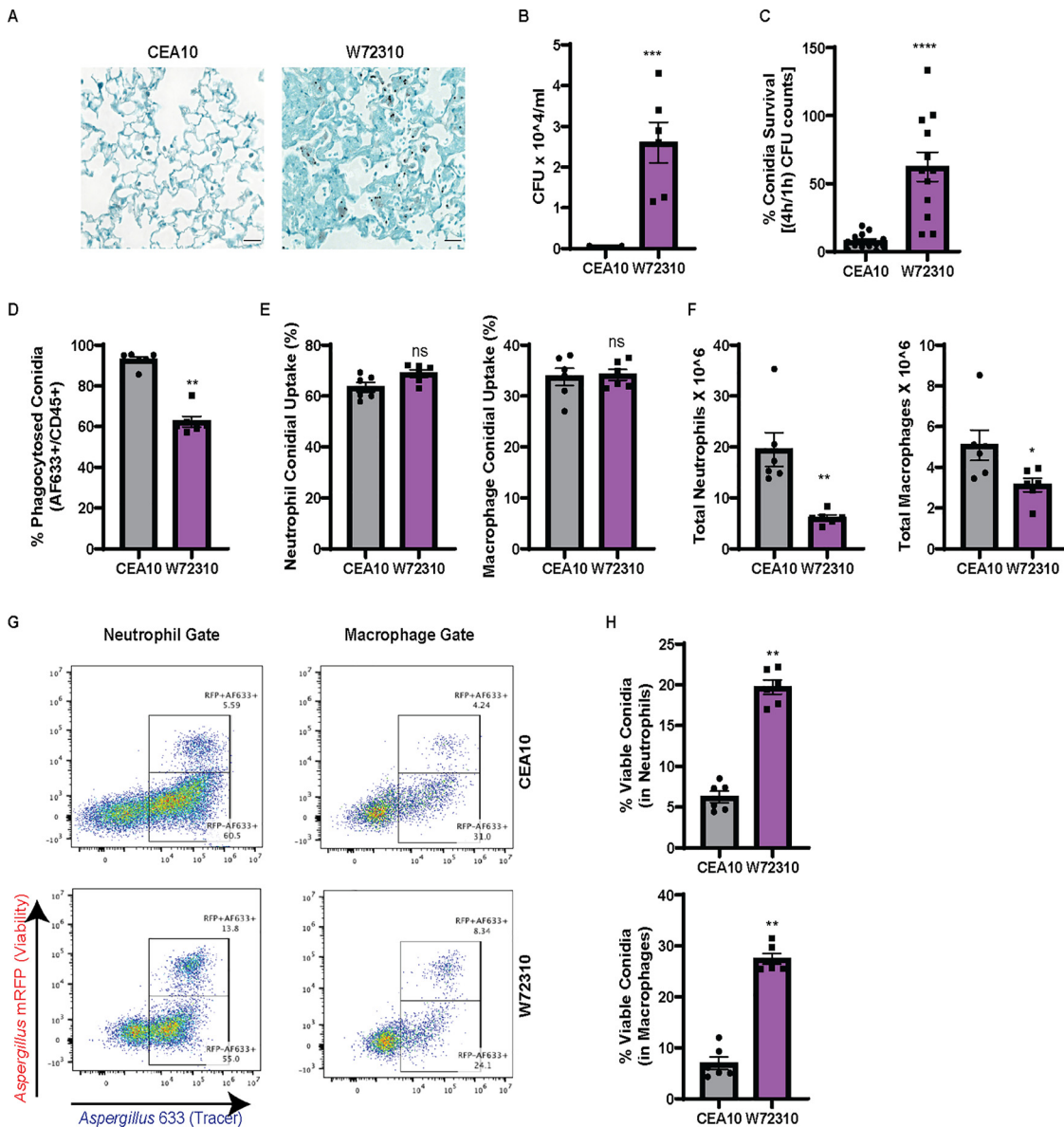
FIG 1 *A. fumigatus* clinical isolate W72310 persists longer in the murine lung and is resistant to leukocyte-mediated death compared to the common laboratory strain CEA10. (A) C57BL/6 mice were intranasally inoculated with 1×10^7 live CEA10 or W72310 conidia and euthanized after 7 days. Lungs were fixed in formalin and stained for fungi (GMS stain, black). $n = 6$ to 8 animals, scale bars = 100 μm, 40×. (B) Lungs from parallel experiments were assessed for total CFU ($n = 6$ to 8 animals). (C) CEA10 and W72310 live conidia were incubated with primary bone marrow-derived macrophages for 1 or 4 h, and CFU were quantified. Data are represented as percent survival of 4 h/1 h. Data include 3 independent experiments. C57BL/6 mice were oropharyngeally inoculated with 3.0×10^7 AF633-stained mRFP-CEA10 or mRFP-W72310 conidia for 36 h. (D to F) Lungs were analyzed by flow cytometry for percent phagocytosis of conidia in immune cells (AF633$^+$/CD45$^+$) (D), percent positive conidia (AF633) in neutrophils and macrophages (E), and total neutrophils (CD45$^+$/Ly6G$^+$/CD11b$^+$) and macrophages (CD45$^+$/Ly6G$^-$/CD11b$^+$/CD64$^+$) (F). (G and H) Viability of conidia phagocytosed in neutrophils and macrophages was analyzed by flow cytometry (G) and quantified (H). Representative micrographs were selected out of 6 mice per group. Mann-Whitney single comparisons were used. ns, $P > 0.05$; *, $P \leq 0.05$; **, $P \leq 0.01$; ***, $P \leq 0.001$.

observed in W72310-inoculated animals, no hyphal growth was visible across multiple independent histopathology sections. In a parallel experiment, quantification of total CFU revealed viable fungi only from lungs inoculated with W72310 (Fig. 1B), indicating W72310 persists longer than CEA10 in C57BL6/J mice.

To address how W72310 conidia persist in the lung, we assayed the susceptibility of W72310 and CEA10 fungal conidia to killing by bone marrow-derived macrophages

(BMDMs) *ex vivo*. After incubation of either W72310 or CEA10 conidia with BMDMs for 4 h, W72310 conidial survival was 6-fold higher than CEA10 (Fig. 1C). In order to test this observation *in vivo*, CEA10 and W72310 that ectopically express monomeric red fluorescent protein (mRFP) were generated in order to distinguish live (mRFP$^+$) from dead (mRFP$^-$) conidia by flow cytometry. Given the relatively short half-life of RFP (approximately 45 min) in the phagolysosome of leukocytes, this fluorescent protein functioned as a fungal viability marker during cellular interactions with leukocytes. A fluorescent tracer dye (Alexa Fluor 633 [AF633]) was covalently attached to the surface of the mRFP-expressing strains and served as a conidial tracer (21). We utilized this assay to quantify leukocyte uptake and viability of W72310 and CEA10 conidia in the murine lung. At 36 h after inoculation with AF633-stained mRFP-CEA10 or W72310 conidia, the percentage of W72310 conidia that were phagocytosed by CD45$^+$ immune cells was 30% less than the percentage of CEA10 conidia in CD45$^+$ immune cells (Fig. 1D). However, comparison of neutrophil and macrophage conidial uptake (% positive AF633) showed no difference between CEA10 and W72310 (Fig. 1E). The reduced phagocytosis of W72310 conidia correlated with a 4-fold reduction in neutrophils and 2-fold reduction in total macrophages in the lungs of mice inoculated with W72310 compared to CEA10 (Fig. 1F). The percentage of viable W72310 conidia phagocytosed by neutrophils and macrophages significantly increased 4-fold in comparison to CEA10 (Fig. 1G and H). Taken together, these data suggest the *A. fumigatus* strain W72310 recruits fewer inflammatory cells and is killed less efficiently than the highly virulent CEA10 strain in a murine model of fungal bronchopneumonia.

Comparison of W72310 sensitization to CEA10 sensitization in the murine lung. Given the persistent presence of the W72310 strain in the murine lung, its increased resistance to leukocyte-mediated killing, and the altered cellular response to W72310 conidia, we next compared the overall immune responses to sensitization with CEA10 and W72310 live conidia. Animals were intranasally inoculated and sensitized to W72310 or CEA10 conidia as indicated (Fig. 2A). Compared to phosphate-buffered saline (PBS)-sensitized animals, CEA10 and W72310 animals had 6- and 8-fold-increased serum IgE, respectively (Fig. 2B). Although we observed a trend for more total IgE in animals exposed to W72310 compared to CEA10, the difference was not statistically significant. Additionally, small but detectable CFU were observed in lungs sensitized with CEA10; however, approximately 10^6 CFU were detected in lungs of animals sensitized with W72310 (Fig. 2C). In parallel, total RNA was extracted from whole lungs and analyzed for changes in mRNA levels of immune-related genes using NanoString nCounter technology. As expected, overall changes in mRNA levels were strikingly different in PBS-sensitized animals compared to the two fungal strains (Fig. 2D). Increased signatures in pathways related to cytokine/chemokine signaling, host-pathogen interactions, and innate and adaptive immune signaling were observed in fungal challenged animals as expected (Fig. 2E). Interestingly, the only immune-related pathways with reduced mRNA levels in fungus-exposed mice compared to PBS were transforming growth factor β (TGF-β) and inflammasome-encoding genes (Fig. 2E). Using GO-term analysis with a cutoff of $P \leq 0.01$ to differentiate highly significant pathways in the W72310-sensitized lung compared to PBS, analysis showed prevalent eosinophil, monocyte, and lymphocyte chemotaxis, ERK1 and ERK2 signaling, interferon gamma (IFN-γ) response signaling, and general immune system responses (Fig. 2F). Comparison of PBS- and W72310-sensitized lungs revealed 174 increased and 38 decreased mRNA transcripts (Fig. 2G). Surprisingly, transcripts of only 9 genes were differentially abundant (2-fold or higher) between CEA10- and W72310-challenged mice. Of these, transcripts of all 9 genes were increased in W72310-sensitized animals compared to CEA10-sensitized animals (Fig. 2H). These differentially expressed transcripts are encoded by the genes *nos2*, *clec4e*, *cxcl-9*, *cxcl-10*, *ccl4*, *cxcl-11*, *klra21*, *cxcl3*, and *tnfα*, transcripts largely involved in T cell/monocyte recruitment and activation, host defense, and CXCR3 receptor activation. The lack of differences between CEA10- and W72310-challenged animals seems especially striking given the clear differences in persistent fungal burden.
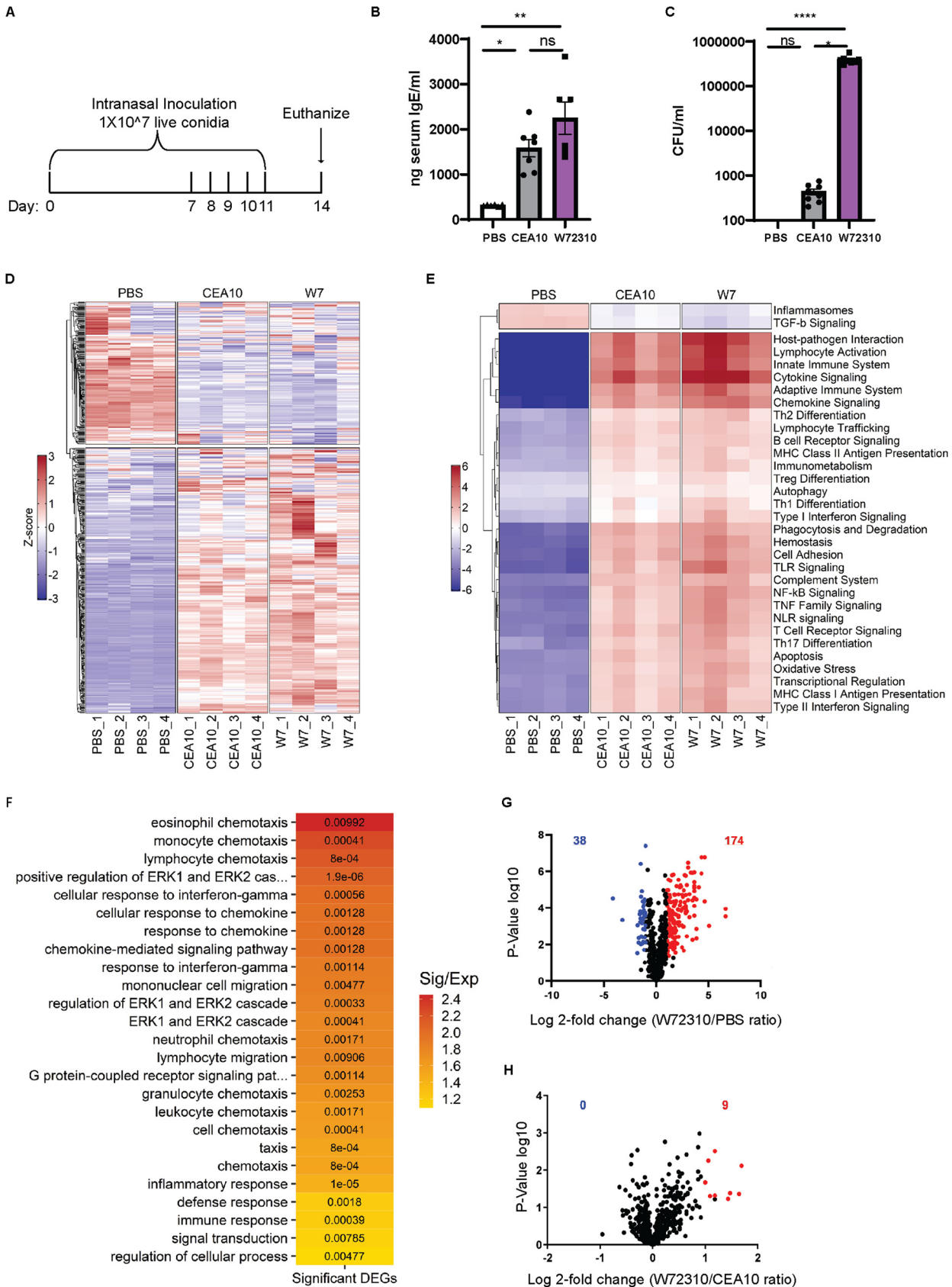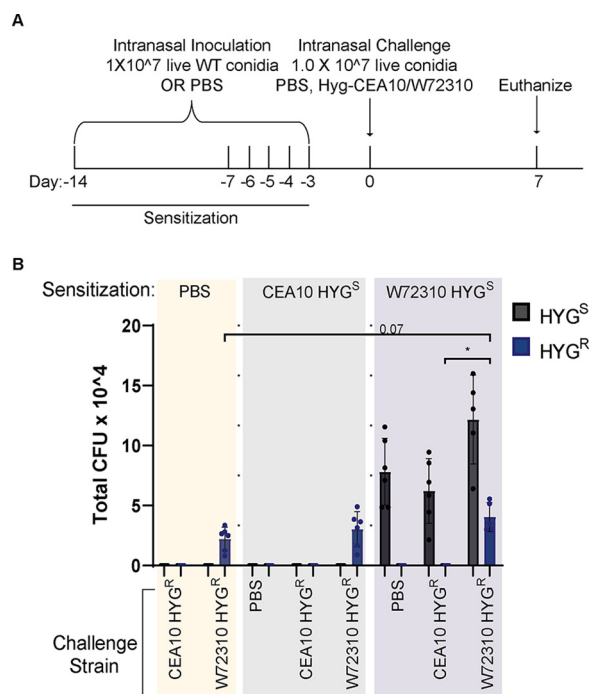
FIG 2 W72310-induced sensitization is similar to CEA10-induced sensitization in the murine lung. (A) Mice were inoculated with either PBS or 1 × 10^7 live W72310/CEA10 conidia on the indicated days and euthanized on day 14. (B) Total serum IgE was measured by ELISA on blood

(Continued on next page)

W72310 accumulates in the murine lung during sensitization. ABPA patients are sensitized to *A. fumigatus* antigens (22). A previous report demonstrated that fungi could persist longer in an allergen-sensitized murine lung than a control lung (23), so we next determined whether sensitization with W72310 or CEA10 increased persistence of a subsequent exposure to W72310 or CEA10 conidia. In light of the data from the immunocompetent murine model (Fig. 1), it is likely that W72310 sensitization alone would cause an accumulation of fungi in the lung, so in order to differentiate between fungi present from sensitization and fungi present due to challenge, we generated CEA10 and W72310 strains that were resistant to hygromycin. Mice were sensitized with either PBS, wild-type (WT) CEA10, or WT W72310 and challenged with either PBS, W72310-hyg, or CEA10-hyg. CFU were measured on Sabouraud dextrose agar (SAB)-containing plates (total CFU) or SAB/hygromycin-containing plates ("challenge" CFU) from the lungs of mice euthanized 7 days after challenge (Fig. 3A). Interestingly, no live conidia were detected in mice sensitized with CEA10 and challenged with PBS, demonstrating that repeated intranasal (i.n.) inoculation was not sufficient to drive CEA10 fungal conidia accumulation in the murine lung (Fig. 3B). In contrast, approximately 1×10^7 live conidia were detected from mice sensitized with W72310 and challenged with PBS, indicating an accumulation of viable fungi in the lung from repeated W72310 i.n. sensitizations (Fig. 3B). Challenge with CEA10-hyg in W72310-sensitized mice did not facilitate persistence of CEA10; however, an almost 2-fold increase in CFU was observed in W72310-challenged mice when sensitized with W72310 but not CEA10 (Fig. 3B). Collectively, these data indicate that sensitization causes a modest increase in persistence of W72310 but not CEA10. Consequently, fungal sensitization itself is not sufficient or necessary to promote fungal persistence in the lung with all strains of *A. fumigatus*.

Sensitization and challenge with W72310 cause increased fungal persistence in the lung in association with increased serum IgE. To determine whether W72310 persists long-term in the mouse lung, we sensitized animals as described for Fig. 2 and subsequently "challenged" mice with another fungal dose on day 0 (Fig. 4A). As a control, animals were sensitized to PBS only and challenged with one dose of W72310 on day 0. To determine fungal persistence, CFU were chosen for quantitation despite the filamentous morphology of *A. fumigatus* because hyphal elements could not be observed in histopathology samples at any time point. Total CFU increased in the lungs of animals sensitized and challenged with W72310 at 2, 7, and 21 days postchallenge in comparison to PBS-sensitized controls (Fig. 4B). This significance was not observed in lungs 28 days postchallenge. CFU were detected 2 and 7 days postchallenge in the PBS-sensitized control group. Surprisingly, CFU were still detectable 21 and 28 days postchallenge in this group as well, although to a much lesser extent. Fixed lungs were stained for fungi (GMS) to observe the fungal presence and morphology. At 2 and 7 days postchallenge in both PBS- and W72310-sensitized mice, prominent conidia were visible (Fig. 4C). Despite the quantification of detectable CFU in PBS-sensitized mice 21 and 28 days postchallenge, conidia were not visible by GMS stain after 7 days (Fig. 4C). Conidia were strongly visible 21 days after challenge in the W72310-sensitized mice; however, they appeared to be taken up in large vacuolar phagocytes (Fig. 4C). Interestingly, multiple conidia were visible in a single host cell. Conidia were mostly

FIG 2 Legend (Continued)
samples collected from animals. $n = 6$ to 7 mice. (C) Total CFU were measured in the lungs of mice. $n = 8$ mice. Mann-Whitney test with Dunn's multiple comparison was used. *, $P \leq 0.05$; **, $P \leq 0.01$; ***, $P \leq 0.001$; ****, $P \leq 0.0001$. (D) Total mRNA was extracted from the whole lung, and gene expression was analyzed by NanoString nCounter immunology panel. Downregulation (blue) or upregulation (red) of individual replicates was represented by heatmap; $n = 4$ mice/group. (E) Pathway signature of mice sensitized to either PBS, CEA10, or W72310. (F) Heatmap showing the degree of enrichment and P value for each GO-term enriched in increased genes. The color of each tile indicates the $\log_2$-transformed degree of enrichment for a given term within each gene set. The P value is overlaid in text to show the significance of each term. The terms on the y axis are ordered according to decreasing degree of enrichment from top to bottom. (G) Volcano plot showing the distribution of fold changes in gene expression in W72310-treated mice compared to PBS: genes with absolute fold changes ≤ 2 and with P value ≤ 0.05 (Student's t test) are shown in blue, and genes with absolute fold changes ≥ 2 and with P value ≤ 0.05 (Student's t test) are shown in red. (H) Volcano plot showing the distribution of fold changes in gene expression in W72310-treated mice compared to CEA10: genes with absolute fold changes ≥ 2 and with P value ≤ 0.05 (Student's t test) are shown in red.
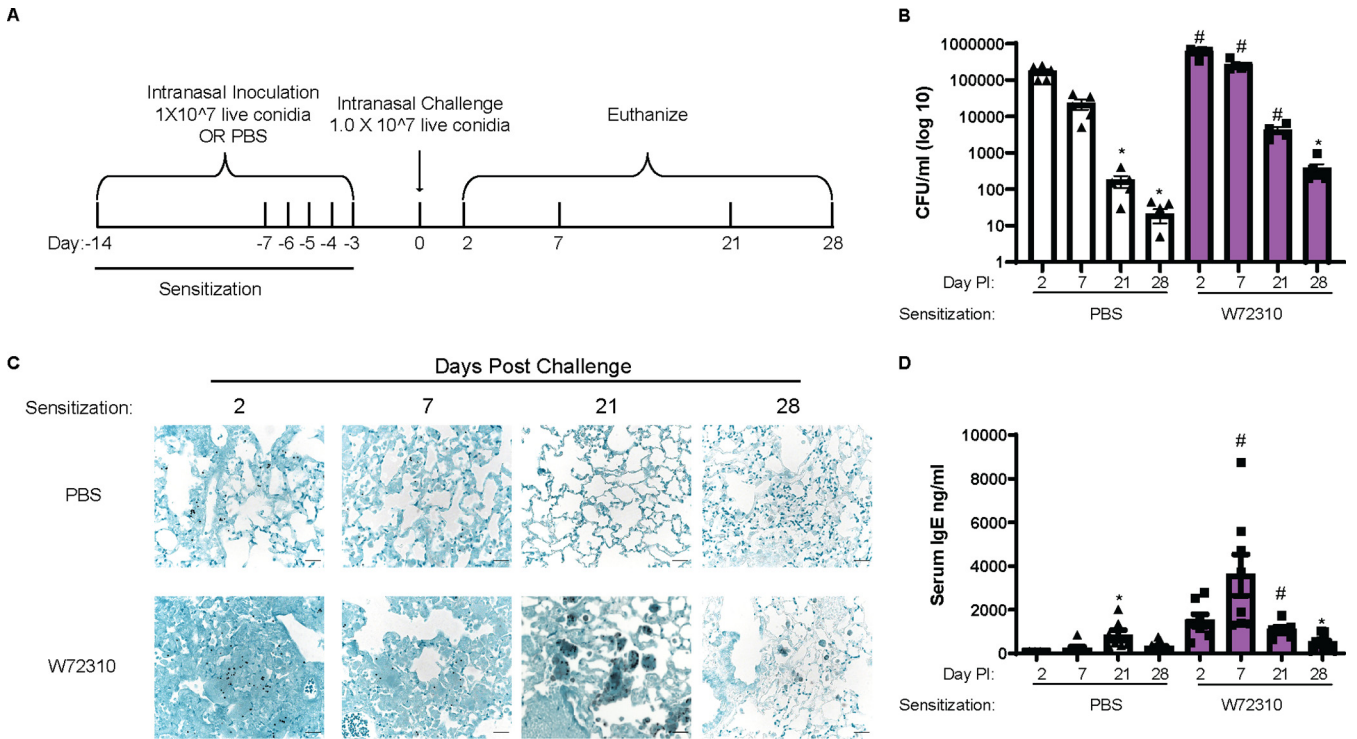
FIG 3 W72310 accumulates in the mouse lung during sensitization. (A) C57BL/6 mice were inoculated with either PBS or 1×10^7 live W72310/CEA10 conidia on the indicated days (sensitization) and challenged on day 0 with either PBS, Hyg-CEA10, or Hyg-W72310; animals were euthanized 7 days after challenge. (B) Lung homogenates were spread on plates containing SAB alone or SAB plus hygromycin and quantified for total CFU. "Challenge" CFU were identified as colonies grown on hygromycin plates, and "Sensitization" CFU were calculated by subtracting hygromycin CFU values from total CFU values (SAB-alone plates). HYG^S, hygromycin-sensitive; HYG^R, hygromycin resistant. n = 6 to 12 mice per group. Mann-Whitney test with Dunn's multiple comparison was used. *, $P \leq 0.05$.

nondetectable by 28 days, with a small number visible by GMS stain. Collectively, these data demonstrate that W72310 can persist in a fungus-sensitized murine lung up to 1 month after inoculation.

Blood was collected from each animal, and total serum IgE levels were measured by enzyme-linked immunosorbent assay (ELISA) to determine the overall allergic response. As expected, total IgE levels increased 2 and 7 days postchallenge in W72310-sensitized mice compared to controls (Fig. 4D); however, significant increases were not detected at 21 and 28 days. Interestingly, even in the PBS-sensitized animals, total serum IgE was increased at 21 days compared to PBS-sensitized control at 2 days. Overall, these data indicate that sensitization and challenge with strain W72310 maintain high levels of IgE.

Sensitization and challenge with W72310 cause increased inflammation, leakage, and mucous cell metaplasia. Eosinophilia is a hallmark of ABPA disease (24). Differential staining of airway/bronchoalveolar lavage (BAL) fluid cells revealed that eosinophils were increased 2, 7, and 21 days after sensitization and challenge with W72310 live conidia in comparison to PBS-sensitized controls (Fig. 5A). Moreover, macrophages and lymphocytes were increased at all time points (Fig. 5A). Interestingly, lymphocytes and eosinophils continued to be detectable 28 days postchallenge but at lower levels. Overall neutrophils decreased over time, but no significant differences were observed between control and experimental groups at any time points (Fig. 5A). The inflammatory response was also assessed by staining lung sections for hematoxylin and eosin (H&E). Some cellular infiltrates were observed in PBS-sensitized mice 2 and 7 days postchallenge with W72310, while robust inflammation, including eosinophils, was observed in animals sensitized and challenged with W72310 at all time points (Fig. 5B). Furthermore, animals sensitized and challenged with W72310 for all time points had detectable mucous cells in airways as shown by periodic acid-Schiff
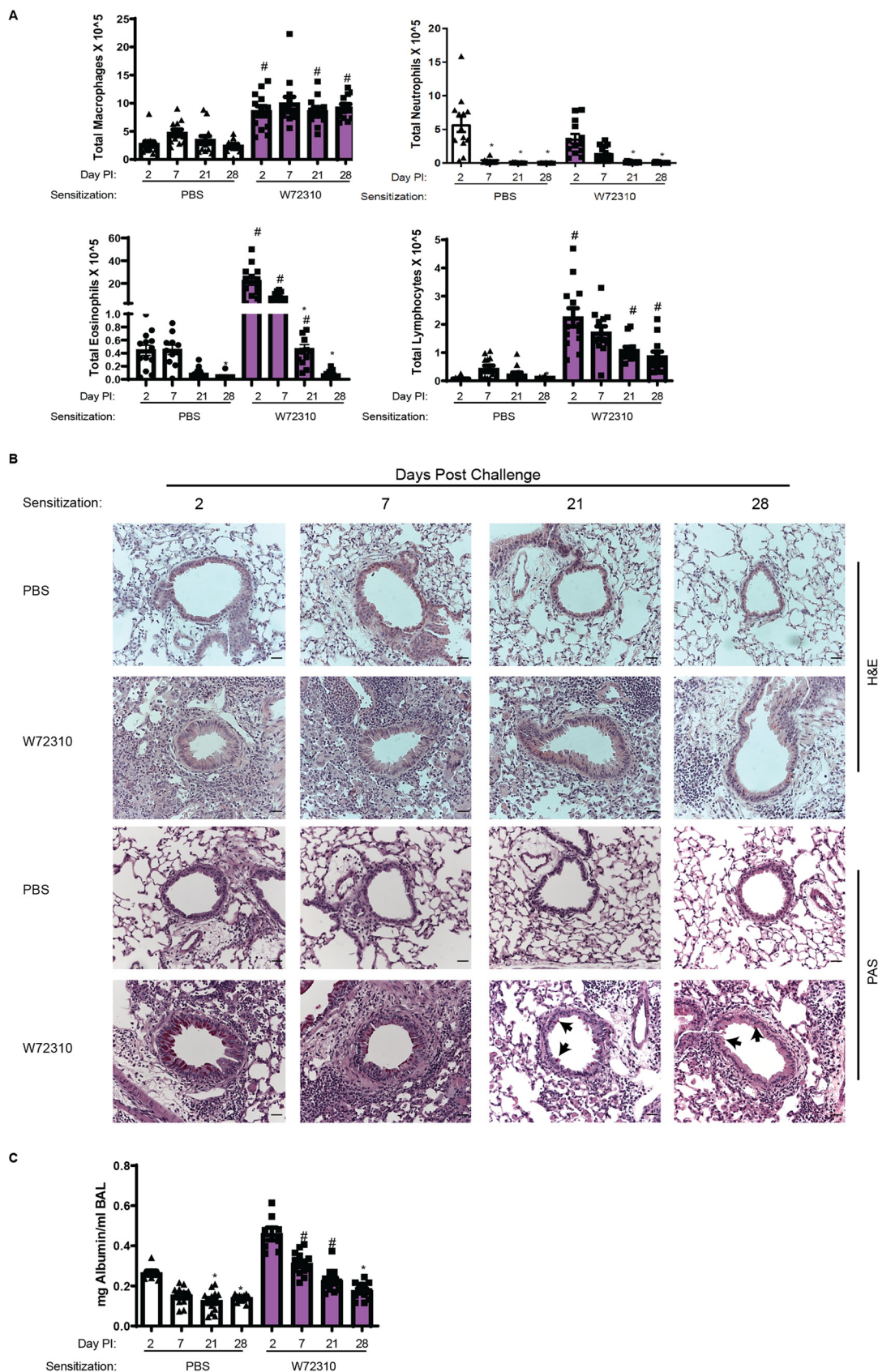
FIG 4 Sensitization and challenge with W72310 causes increased fungal persistence in the lung in association with increased serum IgE. (A) Schematic of ABPA model protocol. C57BL/6 mice were inoculated with either PBS or 1×10^7 live W72310 conidia on the indicated days and challenged on day 0. Animals were subsequently euthanized on days 2, 7, 21, and 28. (B) CFU were quantified from total lung homogenates at the indicated time points and represented on a log scale. (C) Paraffin-embedded fixed lungs were stained with GMS, and images were captured at 40×; scale bar = 100 μm. (D) Total serum IgE was measured by ELISA on blood samples collected from animals. (B and D) Kruskal-Wallis with Dunn's comparison to 2-day time point (within same sensitization protocol): *, ≤0.05. Kruskal-Wallis with Dunn's comparison to same time point (within different sensitization protocol): #, ≤0.05. Data include 2 independent experiments and $n = 8$ to 12 mice.

(PAS)-stained lung sections (Fig. 5B, black arrows). At early time points, 2 and 7 days after challenge, there were a large number of mucus-producing cells, which persisted at lower levels at later time points.

Total albumin in the BAL fluid was measured to evaluate the extent of vascular leakage and potential damage to the lungs in the airways. Quantification of albumin showed significant increases in animals sensitized and challenged with W72310 at 7 and 21 days compared to PBS-sensitized controls, indicating airway damage that resolved by day 28 (Fig. 5C).

Mice recall challenged with W72310 have increased airway inflammation and damage in the lungs. Major features of ABPA disease are periods of remission and exacerbation (25). To determine if mice with persistent W72310 in the lungs were susceptible to a recall response, mice were sensitized and challenged with either PBS or W72310 and 21 days after challenge all animals were recall challenged with either PBS or W72310 live conidia (Fig. 6A). We chose to rechallenge mice at 21 days after the initial challenge because we wanted to use a time point in which conidia had been persistent long-term but were still highly prevalent. This was in order to determine if the presence of conidia themselves could maintain an environment in the lung prone to "exacerbations." BAL fluid and lung suspension neutrophils and eosinophils were significantly increased in the W72310 recall-challenged group compared to the PBS recall-challenged group (Fig. 6B). Serum IgE levels were increased 5-fold in mice sensitized and challenged with W72310 at 21 days compared to PBS-sensitized challenged mice, as would be expected (based on results from the time course [Fig. 4D]), and BAL fluid albumin was measured in order to assess damage and leakage in the airways (Fig. 6C). Total albumin levels were increased 2-fold in the airways of mice sensitized, challenged, and recall challenged with W72310 compared to both PBS controls. Th2

A

B

C

FIG 5 Sensitization and challenge with W72310 cause increased pulmonary inflammation, leakage, and mucous cell metaplasia. (A) Total BAL fluid was quantified for individual cell populations of macrophages, neutrophils, lymphocytes, and

(Continued on next page)

cytokines IL-4/IL-10 and Th1 cytokine IFN-γ were significantly increased in BAL fluid of mice sensitized, challenged, and recall challenged with W72310 compared to PBS controls (Fig. 6D). IL-17A cytokine levels were not detectable (data not shown). Collectively, these data demonstrate that W72310 persists for several weeks in a fungus-sensitized murine lung and elicits strong inflammation, damage, mucus production, and an exacerbation-like immune response.

Comparison of W72310 and CEA10 whole-genome sequences. Given the clear differences in immune response to CEA10 and W72310, we wanted to address potential fungus-mediated mechanisms for these observations. As a first step toward understanding the fungal contribution to these responses, whole-genome sequencing of CEA10 and W72310 was conducted. Sequencing and variant analysis revealed a total of 56,036 variants in W72310 that differed from the AF293 reference genome, compared to only 13,014 variants identified in CEA10. These variants included 2,392 positions in W72310 and 874 variants in CEA10 for which no allele could be determined (and which possibly represent a deletion at that position compared to the AF293 reference genome). We consequently identified 49,806 variants that were exclusive to W72310 and not shared with CEA10 (18,088 excluding synonymous and intergenic variants), compared to only 8,302 variants found in CEA10 but not present in W72310 (1,922 excluding synonymous and intergenic variants). W72310 also had a greater number of missense variants with a total of 6,486, compared to only 814 in CEA10. Given the differences observed between W72310 and CEA10 in conidial viability, germination rate, and persistence in the lung, we narrowed our focus to nonsynonymous variants unique to W72310 (not present in CEA10) occurring in genes involved in oxidative stress responses, cell wall biology, melanin, and metabolism using reverse GO-term mapping. Variants were identified in 20 unique oxidative stress response genes, 6 cell wall genes, and 6 melanin genes (Table 1). Interestingly, no variants were identified in core metabolism genes. When nonsynonymous variants unique to W72310 were mapped onto putative allergen genes, 184 single nucleotide polymorphisms (SNPs) and indels in 69 unique genes, with mutation load ranging from 1 to 21 variants per gene, were found (Table 2). In order to corroborate differences observed in oxidative stress resistance, mRFP-CEA10 and mRFP-W72310 strains were assayed for susceptibility to oxidative stress-inducing agents, hydrogen peroxide and menadione. The percentage of viable CEA10 conidia (RFP$^+$) was significantly reduced by 50% (hydrogen peroxide) and 40% (menadione), respectively. In contrast, incubation of W72310 with hydrogen peroxide and menadione decreased the percentage of viable conidia by only less than 5% (Fig. 7). Collectively, these data show that W72310 conidia are less susceptible to oxidative stress-induced death than those of CEA10 and this may contribute to its persistent phenotype in the mouse lung. The allele(s) driving this phenotype in W72310 conidia remains to be determined in future studies.

DISCUSSION

In the current study, we characterized a unique clinical strain of *A. fumigatus* which persists in the murine lung and elicits an ABPA-like disease state. By identifying and characterizing the W72310 strain, our studies demonstrated that an *A. fumigatus* strain can be resistant to immune cell-mediated killing and that it can persist in the murine lung as viable conidia while eliciting a strong IgE/inflammatory/damage response. These data are important because they suggest *A. fumigatus* strains exist in the population that can persist in mammalian airways and induce pathological immune responses without robust fungal growth. Moreover, our data provide an opportunity to uncover

FIG 5 Legend (Continued)
eosinophils. (B) Paraffin-embedded fixed lungs were stained with H&E and PAS, and images were captured at 20×; scale bar = 100 μm. (C) BAL supernatant was analyzed for total concentrations of albumin. (A and C) Kruskal-Wallis with Dunn's comparison to 2-day time point (within same sensitization protocol): *, ≤0.05. Kruskal-Wallis with Dunn's comparison to same time point (within different sensitization protocol): #, ≤0.05. Data include 2 independent experiments and n = 8 to 12 mice.

A
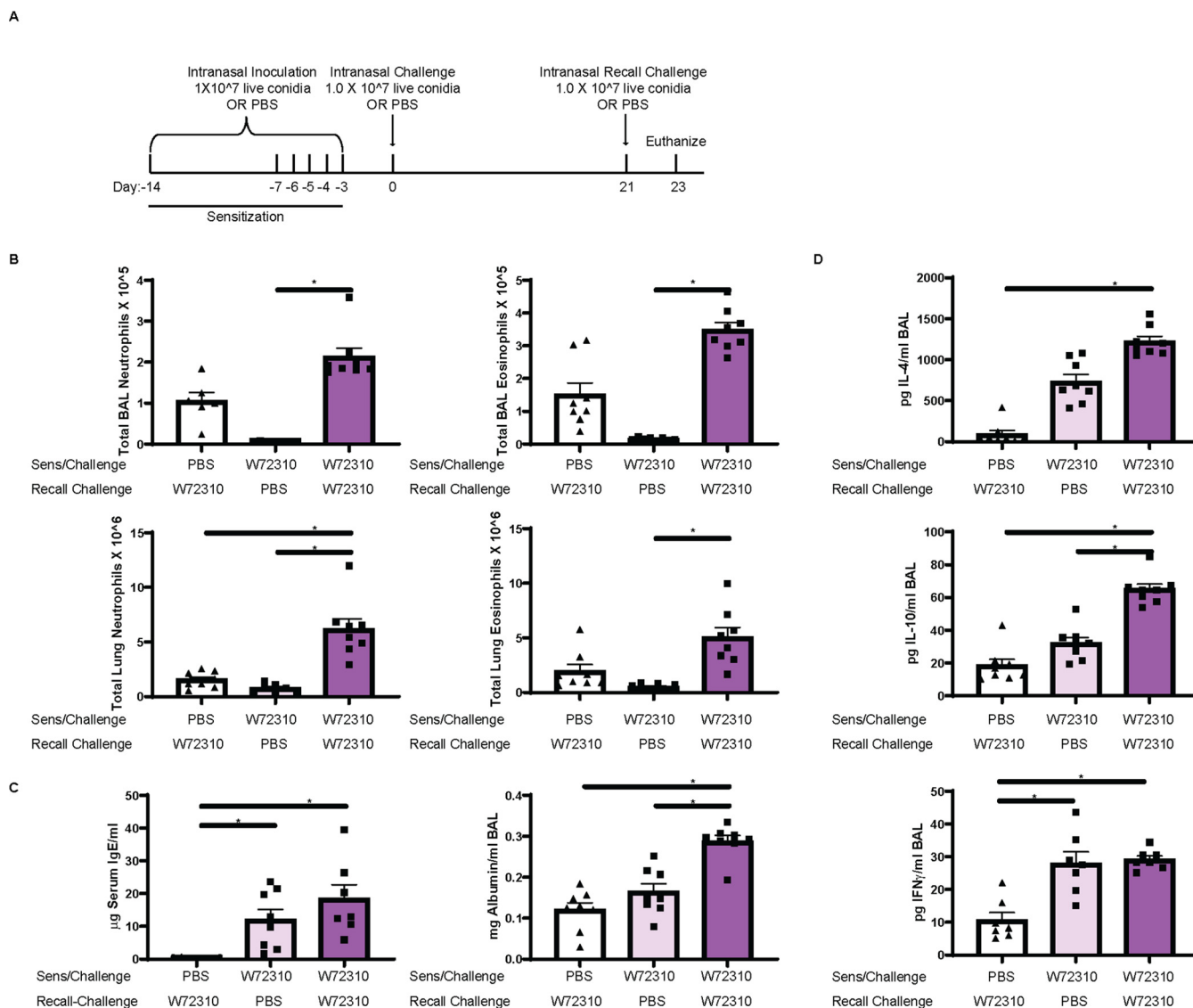
FIG 6 Sensitization and challenge with W72310 and subsequent recall challenge cause increased tissue inflammation, damage, Th1/2, and IgE response. (A) Schematic of ABPA exacerbation protocol. C57BL/6 mice were inoculated with either PBS or 1×10^7 live W72310 conidia on the indicated days (sensitization and challenge) and recall challenged 21 days after initial challenge. Animals were subsequently euthanized 48 h later. (B) Neutrophils (CD45$^+$/SiglecF$^-$/Ly6G$^+$/CD11b$^+$) and eosinophils (CD45$^+$/SiglecF$^+$/CD11c^{low}) were quantified by flow cytometry in BAL fluid and lung suspensions. (C) Serum was isolated from mice, total IgE levels were quantified, and BAL supernatant was analyzed for total albumin. (D) BAL supernatant IL-4, IL-10, and IFN-γ were measured. Mann-Whitney test with Dunn's multiple comparison was used. *, $P \le 0.05$.

novel fungal contributions to allergy-like diseases due to the long-term persistence of W72310 conidia in murine lungs.

We hypothesize that a key fungal mechanism for fungal persistence is enhanced oxidative stress resistance of the W72310 conidia. Reactive oxygen species (ROS) generated by NADPH-oxidases in neutrophils and macrophages are critical components in host defense against *A. fumigatus* infection (26, 27). Intriguingly, our data demonstrate that W72310 conidia are more resistant to both hydrogen peroxide- and menadione-induced death than CEA10 conidia (Fig. 7). Moreover, neutrophils and macrophages have reduced killing of W72310 conidia compared to CEA10 conidia (Fig. 1G). Genome sequencing revealed that W72310 has 20 oxidative stress response genes with high-impact SNPs (Table 1). Of particular interest, perhaps, the catalase Afu6g03890/*catA* has 6 variants in W72310 and not CEA10 (Table 1). Previous studies demonstrated that a catalase mutant generated in *A. fumigatus* was more sensitive to hydrogen peroxide. Interestingly, its conidia did not have any

TABLE 1 Nonsynonymous variants found in W72310 relative to AF293 that are not found in CEA10 (O_2 stress, cell wall, and melanin genes)

	Gene ID	No. of exclusive variants	Annotation
O_2 stress	Afu2g01520	10	Ortholog(s) has role in ascospore formation, hyphal growth, response to oxidative stress, sporocarp development involved in sexual reproduction
	Afu3g10530	6	Putative protein serine/threonine kinase
	Afu6g03890	6	Spore-specific catalase
	Afu2g04680	5	Protein serine/threonine kinase
	Afu4g10770	5	Psi-producing oxygenase A
	Afu5g11820	5	Ortholog(s) has cytosol, nucleus localization
	Afu6g12522	5	Putative transcription factor and response regulator of a two-component signal transduction system
	Afu2g00200	4	Ortholog(s) has catalase activity
	Afu1g13600	3	Ortholog(s) has cyclin-dependent protein kinase activating kinase activity, cyclin-dependent protein serine/threonine kinase regulator activity, protein serine/threonine kinase activity
	Afu3g12670	3	Putative serine/threonine protein kinase
	Afu4g09110	3	Putative cytochrome *c* peroxidase
	Afu2g01700	2	Ortholog(s) has AMP-activated protein kinase activity, ARF guanyl-nucleotide exchange factor activity
	Afu3g02270	2	Mycelial catalase
	Afu4g00180	2	Fatty acid 8,11-diol synthase
	Afu7g03720	2	Ortholog(s) has RNA polymerase II carboxy-terminal domain kinase activity, cyclin-dependent protein kinase activating kinase activity, cyclin-dependent protein serine/threonine kinase activity
	Afu1g01980	1	Ortholog(s) has role in hyphal growth, response to cold, response to heat, response to oxidative stress, response to salt stress, sporocarp development involved in sexual reproduction
	Afu1g05930	1	Ortholog(s) has protein serine/threonine kinase activity
	Afu3g12120	1	Putative fatty acid oxygenase
	Afu5g08580	1	Putative alpha-1,6-mannosyltransferase that initiates the linkage of the N-glycan outer chain
	Afu5g09240	1	Cu/Zn superoxide dismutase
Cell wall	Afu1g13670	5	Conidial cell wall protein A
	Afu6g08510	5	Putative cell wall biosynthesis protein
	Afu3g07650	4	Has domain(s) with predicted pectinesterase activity, role in cell wall modification and cell wall localization
	Afu2g03120	2	Putative cell wall glucanase
	Afu4g03240	2	Putative cell wall galactomannoprotein
	Afu8g06880	2	Ortholog(s) has pectinesterase activity and role in pectin catabolic process
Melanin	Afu2g04200	9	4-Hydroxyphenylpyruvate dioxygenase involved in the L-tyrosine degradation pathway
	Afu1g16590	7	Putative C_2H_2 transcription factor
	Afu1g15440	4	Putative alpha(1-3) glucan synthase
	Afu2g17550	1	Heptaketide hydrolyase ayg1
	Afu2g17560	1	1,3,6,8-Tetrahydroxynaphthalene reductase arp2
	Afu2g17600	1	Conidial pigment polyketide synthase alb1

difference in susceptibility to immune-cell-mediated killing and had similar pathogenicity in mouse models of aspergillosis as did wild-type controls (28–30). Since there are 20 oxidative stress response genes with variants in the W72310 strain, it seems likely that more than one gene/mechanism is involved in its defense against ROS-induced killing. However, we cannot rule out that novel alleles of genes like *catA* encode proteins with increased activity.

Another fungus-centric striking observation from our studies is that W72310 persists in the mouse lung largely as viable conidia. Based on the histology at 21 days postchallenge (Fig. 4C), we observed that the majority of conidia appear to be phagocytosed by large macrophage-like cells. Previous histological analyses of invasive aspergillosis patients have also demonstrated the presence of multiple conidia per giant cell (31); however, the viability of the fungus is not known. Case reports often show *A. fumigatus* in the lung as germlings or hyphae by GMS stain (32), but it is not known whether conidia, germlings, hyphae, or some combination contribute to ABPA and fungal allergic disease pathogenesis. Given that W72310 has previously been shown to have reduced germination rates in comparison to other strains (19, 20), another explanation for its persistence is that remaining in its conidial form does not

TABLE 2 Nonsynonymous variants found in W72310 relative to AF293 that are not found in CEA10 (allergen genes)

| Gene ID	No. of exclusive variants	Annotation
Afu1g02980	21	Putative 6-phosphogluconolactonase
Afu7g05740	10	Putative NAD-dependent malate dehydrogenase
Afu5g11320	9	Allergen Asp f 29
Afu5g04170	6	Heat shock protein
Afu1g14560	5	Putative 1,2-alpha-mannosidase
Afu2g01010	5	Putative myo-inositol-phosphate synthase
Afu2g01170	5	1,3-Beta-glucanosyltransferase with a role in elongation of 1,3-beta-glucan chains
Afu3g11690	5	Putative class II fructose-bisphosphate aldolase
Afu1g09470	4	Putative class V aminotransferase
Afu1g09670	4	Putative HLH transcription factor
Afu2g13530	4	Putative translation elongation factor EF-2 subunit
Afu3g00590	4	Asp-hemolysin
Afu4g01290	4	Glycosyl hydrolase family 75 chitosanase
Afu6g10300	4	Allergen Asp f 28
Afu1g14570	3	Putative phosphoribosyl-AMP cyclohydrolase
Afu2g03830	3	Allergen Asp f 4
Afu2g09960	3	Putative mitochondrial Hsp70 chaperone
Afu3g01110	3	Putative GMP synthase (glutamine-hydrolyzing)
Afu4g10130	3	Ortholog(s) has alpha-amylase activity and role in carbohydrate catabolic process
Afu4g11720	3	Putative phosphatidyl synthase
Afu5g09580	3	Conidial hydrophobin
Afu6g04920	3	Putative NAD-dependent formate dehydrogenase
Afu6g10660	3	Putative ATP citrate lyase subunit
Afu7g05720	3	Pyruvate dehydrogenase complex, dihydrolipoamide acetyltransferase component
Afu1g04130	2	FG-GAP repeat protein
Afu2g10100	2	Allergen Asp f 8
Afu2g11150	2	Putative secretory-pathway GDP dissociation inhibitor
Afu2g11260	2	Putative 3-isopropylmalate dehydratase with a predicted role in nitrogen metabolism
Afu2g16820	2	Putative curved DNA-binding protein
Afu3g00600	2	Ortholog of *Aspergillus fumigatus* A1163: AFUB_047840
Afu3g02270	2	Mycelial catalase
Afu3g09320	2	Serine hydroxymethyltransferase
Afu4g03240	2	Putative cell wall galactomannoprotein
Afu4g06670	2	Allergen Asp f 7
Afu4g10460	2	Homocitrate synthase, essential enzyme of the alpha-aminoadipate pathway of lysine biosynthesis
Afu5g05540	2	Putative nucleosome assembly protein
Afu5g09210	2	Autophagic (vacuolar) serine protease
Afu5g13300	2	Putative extracellular aspartic endopeptidase
Afu6g02230	2	Putative glucokinase
Afu6g02280	2	Allergen Asp f 3
Afu6g09690	2	Glutathione *S*-transferase gliG
Afu6g09740	2	Thioredoxin reductase gliT
Afu8g07080	2	Putative secreted metalloprotease
Afu1g02820	1	Putative NADH-quinone oxidoreductase
Afu1g06830	1	Putative 60s acidic ribosomal protein superfamily member
Afu1g07440	1	Molecular chaperone
Afu1g08980	1	UPF0160 domain protein
Afu1g10630	1	Putative *S*-adenosylmethionine synthetase
Afu1g11460	1	Putative 1,3-beta-glucanosyltransferase
Afu2g00690	1	Ortholog(s) has glucan 1,4-alpha-glucosidase activity, role in polysaccharide metabolic process and Golgi apparatus, endoplasmic reticulum, prospore membrane localization
Afu2g06150	1	Putative protein disulfide isomerase
Afu2g12630	1	Allergen Asp f 13
Afu2g13250	1	Putative bifunctional tryptophan synthase
Afu2g15430	1	Sorbitol/xylulose reductase
Afu3g03060	1	Allergen Asp f 34
Afu3g07430	1	Putative peptidyl-prolyl *cis-trans* isomerase
Afu3g10460	1	Putative nuclear transport factor
Afu3g11300	1	Putative proteasome component
Afu3g11400	1	Aspartic acid endopeptidase
Afu4g00610	1	Putative aryl-alcohol dehydrogenase

TABLE 2 (Continued)

Gene ID	No. of exclusive variants	Annotation
Afu4g07410	1	Has domain(s) with predicted catalytic activity
Afu4g07690	1	Putative phosphoribosylaminoimidazole-carboxamide formyltransferase/IMP cyclohydrolase
Afu4g08720	1	Putative secreted phospholipase B
Afu5g06390	1	Putative adenosine kinase
Afu5g10550	1	ATP synthase F1, beta subunit
Afu6g06770	1	Putative enolase
Afu6g11330	1	Ortholog(s) has thiamine phosphate phosphatase activity and role in dephosphorylation, thiamine biosynthetic process
Afu6g12930	1	Mitochondrial aconitate hydratase
Afu8g05020	1	Putative secreted N-acetylhexosaminidase

allow full immune recognition of the fungus. Of note, W72310 elicited less of an inflammatory response than CEA10 in an immunocompetent pulmonary challenge model (Fig. 1E). LC3-associated phagocytosis has been shown to be critical in fungal killing and is dependent on exposure of the fungal cell wall components melanin and β-glucan (33). Sequence analysis showed high-impact SNPs in 6 cell wall genes and 6 melanin genes which could potentially prevent full recognition and/or killing of the fungus (Table 1). Collectively, SNPs in melanin and cell wall stress genes may affect overall germination, and immune cell recognition of W72310 and SNPs in oxidative stress response genes could affect overall viability of phagocytosed W72310 conidia. Rigorous fungal genetic studies will be needed to determine specifically which gene(s) is important overall for the persistent phenotype.

Despite a similar immunological response to sensitization between W72310 and CEA10, select interferon-responsive genes were differentially expressed. CXCR3 was not differentially expressed between W72310 and CEA10 (data not shown); however, expression of its ligands, CXCL-9 and CXCL-10, was higher in W72310-sensitized lungs than in those sensitized to CEA10. CXCL9 and CXCL10, which have been shown to be induced in other mouse models of asthma and *A. fumigatus*-induced inflammation (34–36), activate Th1-type immune responses through CXCR3. Because CXCR3 is preferentially expressed in Th1 cells (37), this could indicate a potential role for the Th1 immune response in the overall persistence observed from W72310. Both in a mouse model of severe asthma and in humans with severe asthma, CXCL-10 was shown to play a critical role in corticosteroid resistance and Th1-mediated inflammation (38).
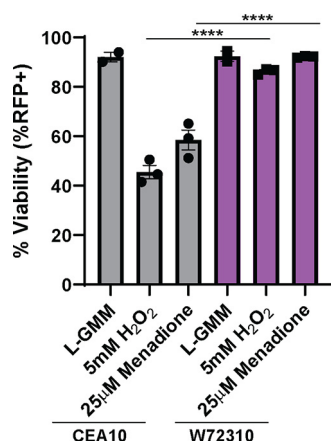
FIG 7 W72310 is more resistant to oxidative stress-induced death than CEA10. mRFP-CEA10 and mRFP-W72310 were incubated with either $25\,\mu$M menadione or $5\,$mM H_2O_2 for 6 h and analyzed by flow cytometry for viability (%RFP$^+$). Data are representative of 3 independent experiments with 3 to 4 technical replicates/experiment. One-way analysis of variance (ANOVA) with Tukey's multiple comparison was used; ****, $P \leq 0.0001$.

However, differences in the immune response at this time point could be in response to either the different strains of fungi or different quantities of fungi, since we observe significantly more W72310 CFU at this time point (Fig. 2C).

The results of our present study indicate that persistent conidial colonization in the fungus-sensitized mouse lung causes many features of APBA-like disease (Fig. 4 and 6). Diagnosis of ABPA has proven to be challenging, and it has long been postulated that ABPA rates are underrepresented due to a lack of consistency in diagnostic methods (22). Elevated total and *A. fumigatus*-specific IgE, *A. fumigatus* cutaneous reactivity, bronchial asthma, airway eosinophilia, and bronchiectasis are the major criteria utilized to diagnose APBA. Our data show increased airway eosinophilia, serum IgE, and albumin in the BAL fluid of mice up to 21 days after challenge with *A. fumigatus*, indicating a pathogenic role for *A. fumigatus* long-term persistence. In other published mouse models of ABPA, repeated inoculation is required for these phenotypes to be maintained (34, 39). Further analysis of airway mechanics, host immunology, and changes in morphology will be needed to determine the extent of ABPA disease-like pathogenesis in animals with a longer-term W72310 infection.

Importantly, ABPA is primarily diagnosed in patients with cystic fibrosis, due to an environment in the lung prone to long-term microbial colonization. Mouse models of CF have also shown a strong role for *A. fumigatus* in CF disease pathogenesis. CF transmembrane conductance regulator (CFTR) knockout (KO) and dF508 mice develop robust inflammatory, IL-4, and IgE (specifically in CD4$^+$ T cells) responses to *A. fumigatus* hyphal extract (40). Additionally, exposure of mice to *A. fumigatus* conidia for 24 to 72 h causes increased inflammation, mucus production, and BAL fluid inflammatory cytokine production in CFTR KO compared to WT mice (41), and increased inflammasome activity was observed in CFTR KO mice in response to *A. fumigatus* conidial exposure (42). Future experiments exposing genetically engineered CF mice to W72310 could provide valuable insight into mechanisms of disease pathogenesis and therapeutic efficacy. These types of studies could be especially critical because the concept that strains of *A. fumigatus* can survive in the lung without germinating but cause ABPA-like disease would significantly affect the types of treatments a patient would receive, including antifungals. Moreover, identification of specific fungal alleles that promote long-term persistence may help diagnose chronic infections in lieu of transient colonization that would help guide antifungal deployment in these at-risk groups, such as CF patients.

MATERIALS AND METHODS

Animal inoculations. Mice were housed in autoclaved cages at ≤4 mice per cage with HEPA-filtered air and water. For single-exposure studies, outbred wild-type C57BL/6 female mice 8 to 12 weeks old (Jackson Laboratories) were intranasally inoculated with 1×10^7 live conidia (in 40 μl PBS) per mouse. *A. fumigatus* strains CEA10 and W72310 were grown on 1% glucose minimal medium (GMM) for 3 days at 37°C, and conidia were collected in 0.01% Tween and washed 3 times in sterile PBS. Animals were inoculated with 3×10^7 live conidia for 36 h (FLARE), 1×10^7 live conidia 1 time in week 1 and 5 times in week 2 (sensitization), and 1×10^7 live conidia on the first day of week 3 (challenge). Animals were monitored daily for disease symptoms, and we carried out our animal studies in strict accordance with the recommendations in the *Guide for the Care and Use of Laboratory Animals* (43). The animal experimental protocol 00002241 was approved by the Institutional Animal Care and Use Committee (IACUC) at Dartmouth College.

Isolation of bone marrow and coculture conditions. After euthanasia, femur and tibia were extracted from 8- to 12-week-old C57BL/6 mice and the bones were flushed with PBS to collect bone marrow-derived cells. After red blood cell lysis, cells were counted and cultured with either mRFP-CEA10 or mRFP-W72310 AF633-stained conidia as described previously (21) for 16 h at a 10:1 multiplicity of infection (MOI) with 10 ng/ml interferon gamma (IFN-γ) and 25 mM hydroxyurea (HU).

***In vitro* conidial killing assay.** Freshly harvested murine BMDMs were dosed to 1×10^6/ml in medium, and 1 ml of the above culture was transferred to each well of a 24-well plate. After an overnight incubation at 37°C with 5% CO$_2$ to allow attachment, the BMDM medium was removed and replaced with 0.5 ml of fresh BMDM medium containing 2×10^6/ml *A. fumigatus* conidia from strains of interest (MOI = 1). After 1 h, unbound/unphagocytosed conidia were removed in all wells by aspirating the BMDM medium and gently washing with 1 ml of PBS for each well. For the 1-h group, 200 μl 0.5% sterile SDS in distilled water was added and incubated for 10 min to lyse the macrophages and conduct serial dilutions in sterile 0.01% Tween 80 in distilled water. For the 4-h group, 0.5 ml BMDM medium was added back and incubated for another 3 h before lysing the SDS solution followed by serial dilutions as

above. All serial dilutions (from 10^1 to 10^5, 100 μl) were pipetted on GMM plates via sterile plate spreaders and incubated for 2 days. Plates containing between 30 and 200 colonies were counted, and the number of viable conidia was calculated. The survival rate of 3-h BMDM killing was calculated by n (4-h group)/n(1-h group).

Hygromycin-resistant and mRFP strain generation. Protoplasts from strains CEA10 and W72310 were generated with *Trichoderma harzianum* (Millipore Sigma) lysing enzyme and transformed ectopically with linear constructs of the *gpdA*-driven *hph* hygromycin resistance gene or H2A:mRFP (CEA10) as previously described (44, 45).

RNA preparation and NanoString analysis. Animals were "sensitized" to either PBS, CEA10, or W72310 as described previously, and lungs were removed at euthanasia for mRNA analysis. Lungs were freeze-dried, homogenized with glass beads using Mini Bead Beater (BioSpec Products Inc., Bartlesville, OK), and resuspended in TRIzol (Thomas Scientific) and chloroform to extract RNA according to manufacturer's instructions. After RNA was assessed for quality, 500 ng of RNA was used per NanoString reaction using the nCounter Mouse Immunology v1 Gene Expression Panel (NanoString). nSolver 4.0 software was used for background subtraction and normalization. nCounter Advanced Analysis 2.0 was used for quality control analysis and pathway analysis. For additional pathway analysis, accession numbers were converted to Entrez IDs via the DAVID Gene Accession Conversion Tool (46, 47). The Entrez IDs were then used to pull GO terms for each gene from the Mouse Genome Informatics' website (http://www.informatics.jax.org/batch). The resulting file was reformatted to fit the TopGO package's requirements for gene ID to GO ID conversion (gene_ID\t GOID1;GOID2;. . .;GOIDX). Genes were classified as increased or decreased based on a 2-fold change cutoff and a P value of $\leq$0.05. Lists of all differentially expressed genes (DEGs), increased DEGs, or decreased DEGs were inserted into separate TopGOdata objects using the gene ID to GO ID conversion file to assign all possible GO terms for each gene. A nodesize cutoff of 10 was used, and a classic Fisher test followed by a Benjamini-Hochberg correction for multiple testing was performed via the TopGO R package (48) to determine enriched GO terms within the data sets. The degree of enrichment was calculated as the number of significant genes divided by the number of genes expected by random chance. Data were plotted via the ggplot2 and ComplexHeatmap (49) packages in R version 3.6.2 (12 December 2019).

CFU. Whole lungs were homogenized in 1 ml sterile PBS using glass beads in a Mini Bead Beater. Serial dilutions (1:10 to 1:1,000) were then spread onto agar plates containing Sabouraud medium or Sabouraud medium containing 175 μg/ml hygromycin and incubated overnight (O/N) at 37°C. Plate dilutions containing 50 to 100 visible colonies were quantified and expressed as a measurement of CFU per milliliter.

Histology: GMS, PAS, and H&E. After euthanasia, cannulas were inserted into trachea and lungs were excised from the body cavity. Lungs were inflated with 10% buffered formalin phosphate for 24 h and stored in 70% ethanol until embedding. Paraffin-embedded sections were stained with hematoxylin and eosin (H&E), Grocott-Gomori methenamine silver (GMS), and periodic acid-Schiff (PAS). Slides were analyzed microscopically with a Zeiss Axioplan 2 imaging microscope (Carl Zeiss Microimaging, Inc., Thornwood, NY) fitted with a QImaging Retiga-SRV Fast 1394 RGB camera.

Serum analysis. Cardiac punctures were performed postmortem. After 1 h at room temperature, blood samples were centrifuged at 2,000 $\times$ g for 30 min, and serum was isolated. Total IgE was measured by ELISA using a kit (Invitrogen) and performed according to the manufacturer's instructions.

BAL analysis (inflammatory cells, albumin, ELISAs). After euthanasia, cannulas were inserted into trachea and lungs were removed. Lungs were lavaged with 3 sequential cold PBS washes (1 ml, 0.5 ml, 0.5 ml). Broncho-alveolar lavage (BAL) fluid was centrifuged at 300 $\times$ g for 5 min, and supernatant was removed for cytokine (IL-4, IL-10, and IFN-γ [R&D]) and albumin (Eagle Diagnostics) analysis according to manufacturer's instructions. Remaining cells were counted and centrifuged onto slides using Rotofix Cytospin. Up to 300 cells were counted to determine percentages of macrophages, neutrophils, eosinophils, and lymphocytes. Total numbers of individual cell populations were calculated using individual percentages multiplied by total BAL cell numbers.

Cell death assay. Liquid GMM was inoculated with 2.0 $\times$ 10^6 mRFP-CEA10 or mRFP-W72310 and incubated with either 25 μM menadione or 5 mM hydrogen peroxide for 6 h at 37°C. After incubation, conidia were run on a Beckman Coulter Cytoflex S flow cytometer for percent positive RFP (viability). Analysis was performed using FlowJo version 9.9.6 as previously described (26).

Flow cytometry and Fluorescence Aspergillus REporter (FLARE) analysis. Whole-lung single-cell suspensions were prepared as described previously (45). Briefly, lungs were minced and digested in buffer containing 2.2 mg/ml collagenase type IV (Worthington), 100 μg/ml DNase I (Zymo Research), and 5% fetal bovine serum (FBS) at 37°C rotating for 45 min. Digested samples were then passed through an 18-gauge needle, resuspended in red blood cell lysis buffer, diluted with PBS, passed through a 100-μm filter, and counted. For flow cytometry analysis, cells were stained with a viability dye (eFluor 780; eBioscience), anti-CD45 (Pacific Orange; Invitrogen), anti-CD11b (PECy5 [BioLegend] for cellularity, PerCPCy5.5 [BioLegend] for FLARE), anti-CD11c (phycoerythrin [PE], BioLegend), anti-Ly6G (fluorescein isothiocyanate [FITC], BioLegend), anti-CD64 (BV421; BioLegend), and anti-SiglecF (BV421; BD Bioscience). Samples were analyzed on a MACSQuant VYB flow cytometer (cellularity) or Beckman Coulter Cytoflex S (FLARE). Macrophages were identified as CD45$^+$/Ly6G$^-$/CD11b$^+$/CD64$^+$, neutrophils were identified as CD45$^+$/SiglecF$^-$/Ly6G$^+$/CD11b$^+$, and eosinophils were identified as CD45$^+$/SiglecF$^+$/CD11c^{low}. Analysis was performed with FlowJo version 9.9.6.

Genome sequencing and variant analyses. Mycelial cultures of *A. fumigatus* using liquid glucose minimal medium with yeast extract were inoculated in small petri dishes grown overnight (18 to 24 h) at 37°C. Mycelia were collected, lyophilized, and bead beaten to powder, and DNA was extracted as previously described (50). Genomic sequencing libraries of the DNA were constructed using the SeqOnce

(SeqOnce Biosciences, Pasadena, CA) with multiplexing barcodes by the Genomics Core at UC Riverside Institute for Integrative Genome Biology. The genomic libraries were sequenced as 2×150-bp reads on an Illumina Novaseq 6000 (Illumina, San Diego, CA) at UC San Francisco Sequencing Core to generate ∼2.17 Gb of sequence. Sequence data for strain CEA10 were obtained from the Sequence Read Archive under accession no. ERR232423 and BioProject PRJEB1497. The sequence reads for each strain were aligned to the Af293 genome downloaded from FungiDB v.46 (51, 52) using BWA v0.7.17 (53) and converted to the BAM file format after running fixmate and sort commands in SAMtools v1.10 (54). Duplicate reads were removed, and reads were indexed using MarkDuplicates and Build BamIndex in Picard tools v2.18.3 (http://broadinstitute.github.io/picard). To avoid overcalling variants near alignment gaps, reads were further realigned using RealignerTargetCreator and IndelRealigner in the Genome Analysis Toolkit GATK v3.7 (55). The variants (SNPs and indels) for W72310 and CEA10 were genotyped relative to the *A. fumigatus* reference genome Af293 using the HaplotypeCaller step in GATK v4.0 (https://doi.org/10.1101/201178). Filtering was accomplished using GATK's SelectVariants call with the following parameters: for SNPs, -window-size = 10, -QualByDept < 2.0, -MapQual < 40.0, -QScore < 100, -MapQualityRankSum < −12.5, -StrandOddsRatio > 3.0, -FisherStrandBias > 60.0, -ReadPosRankSum < −8.0; for indels, -window-size = 10, -QualByDepth < 2.0, -MapQualityRankSum < −12.5, -StrandOddsRatio > 4.0, -FisherStrandBias > 200.0, -ReadPosRank < −20.0, -InbreedingCoeff < −0.8. Resultant variants were annotated with snpEff (56) using the Gene File Format gene annotation for Af293 v.46 in FungiDB. Variants that overlapped transposable elements (TEs) were removed by positional mapping to locations of annotated TEs in the FungiDB v.46 release of the Af293 reference genome, using BEDtools -subtract (57). Mutations in W72310 were analyzed relative to CEA10 using a custom script implemented in the R programming environment (58). To identify mutations occurring in allergen genes, a database of genes putatively capable of eliciting an immune response was curated from the published literature ($n = 113$) (Table 2) and mapped against W72310 variant positions using a custom script in R. Putative allergen genes in W72310 containing variants other than synonymous or intergenic mutations were annotated in Fungi DB v.46 (52). To investigate variants unique to W72310 and occurring in genes relevant to the phenotypes of interest in this study (oxidative stress, cell wall integrity, primary metabolism, and melanin production), we used reverse GO mapping of the terms GO:0006979 (response to oxidative stress), GO:0005618 (cell wall), GO:0044238 (primary metabolic process) GO:0006582 (melanin metabolic process), and GO:0042438 (melanin biosynthetic process).

Statistical analysis. All statistical analyses were performed with Prism 8.3 software (GraphPad Software Inc., San Diego, CA). For *in vitro* comparison of 2 groups, Student's *t* test was used. For animal experiments, nonparametric analyses were performed (Kruskal-Wallis, Dunn's multiple comparisons; Mann-Whitney, single comparisons). All error bars represent standard errors of the means. NS, $P > 0.05$; *, $P \leq 0.05$; **, $P \leq 0.01$; ***, $P \leq 0.001$; ****, $P \leq 0.0001$.

Data availability. Sequence data for W72310 were deposited in the Sequence Read Archive under BioProject no. PRJNA614926. The code and data files for variant assessment associated with this project can be accessed via GitHub in the repository stajichlab/W72310 (https://doi.org/10.5281/zenodo.4116457) (59).

REFERENCES

1. Pashley CH. 2014. Fungal culture and sensitisation in asthma, cystic fibrosis and chronic obstructive pulmonary disorder: what does it tell us? Mycopathologia 178:457–463. https://doi.org/10.1007/s11046-014-9804-y.

2. Haase G, Skopnik H, Groten T, Kusenbach G, Posselt HG. 1991. Long-term fungal cultures from sputum of patients with cystic fibrosis: Langzeitpilzkulturen von Sputen bei Patienten mit zystischer Fibrose. Mycoses 34:373–376. https://doi.org/10.1111/j.1439-0507.1991.tb00797.x.

3. Rapaka RR, Kolls JK. 2009. Pathogenesis of allergic bronchopulmonary aspergillosis in cystic fibrosis: current understanding and future directions. Med Mycol 47(Suppl 1):S331–S337. https://doi.org/10.1080/13693780802266777.

4. Saunders RV, Modha DE, Claydon A, Gaillard EA. 2016. Chronic *Aspergillus fumigatus* colonization of the pediatric cystic fibrosis airway is common and may be associated with a more rapid decline in lung function. Med Mycol 54:537–543. https://doi.org/10.1093/mmy/myv119.

5. Stevens DA, Moss RB, Kurup VP, Knutsen AP, Greenberger P, Judson MA, Denning DW, Crameri R, Brody AS, Light M, Skov M, Maish W, Mastella G, Participants in the Cystic Fibrosis Foundation Consensus Conference. 2003. Allergic bronchopulmonary aspergillosis in cystic fibrosis—state of the art: Cystic Fibrosis Foundation Consensus Conference. Clin Infect Dis 37:S225–S264. https://doi.org/10.1086/376525.

6. King J, Brunel SF, Warris A. 2016. Aspergillus infections in cystic fibrosis. J Infect 72:S50–S55. https://doi.org/10.1016/j.jinf.2016.04.022.

7. Chotirmall SH, McElvaney NG. 2014. Fungi in the cystic fibrosis lung: bystanders or pathogens? Int J Biochem Cell Biol 52:161–173. https://doi.org/10.1016/j.biocel.2014.03.001.

8. Kauffman HF. 2003. Immunopathogenesis of allergic bronchopulmonary aspergillosis and airway remodeling. Front Biosci 8:e190–e196. https://doi.org/10.2741/990.

9. Hayes D, Murphy BS, Lynch JE, Feola DJ. 2010. Aerosolized amphotericin for the treatment of allergic bronchopulmonary aspergillosis. Pediatr Pulmonol 45:1145–1148. https://doi.org/10.1002/ppul.21300.

10. Wark P. 2004. Pathogenesis of allergic bronchopulmonary aspergillosis and an evidence-based review of azoles in treatment. Respir Med 98:915–923. https://doi.org/10.1016/j.rmed.2004.07.002.

11. Urb M, Snarr BD, Wojewodka G, Lehoux M, Lee MJ, Ralph B, Divangahi M, King IL, McGovern TK, Martin JG, Fraser R, Radzioch D, Sheppard DC. 2015. Evolution of the immune response to chronic airway colonization with Aspergillus fumigatus hyphae. Infect Immun 83:3590–3600. https://doi.org/10.1128/IAI.00359-15.

12. Nawada R, Amitani R, Tanaka E, Niimi A, Suzuki K, Murayama T, Kuze F. 1996. Murine model of invasive pulmonary aspergillosis following an earlier stage, noninvasive Aspergillus infection. J Clin Microbiol 34:1433–1439. https://doi.org/10.1128/JCM.34.6.1433-1439.1996.

13. Hogaboam CM, Gallinat CS, Taub DD, Strieter RM, Kunkel SL, Lukacs NW. 1999. Immunomodulatory role of C10 chemokine in a murine model of allergic bronchopulmonary aspergillosis. J Immunol 162:6071–6079.

14. Murdock BJ, Shreiner AB, McDonald RA, Osterholzer JJ, White ES, Toews GB, Huffnagle GB. 2011. Coevolution of T_H1, T_H2, and T_H17 responses during repeated pulmonary exposure to Aspergillus fumigatus conidia. Infect Immun 79:125–135. https://doi.org/10.1128/IAI.00508-10.

15. Kosmidis C, Denning DW. 2015. The clinical spectrum of pulmonary aspergillosis. Thorax 70:270–277. https://doi.org/10.1136/thoraxjnl-2014-206291.

16. Paugam A, Baixench M-T, Demazes-Dufeu N, Burgel P-R, Sauter E, Kanaan R, Dusser D, Dupouy-Camet J, Hubert D. 2010. Characteristics and consequences of airway colonization by filamentous fungi in 201 adult patients with cystic fibrosis in France. Med Mycol 48:S32–S36. https://doi.org/10.3109/13693786.2010.503665.

17. Chen KTK. 1993. Cytology of allergic bronchopulmonary aspergillosis. Diagn Cytopathol 9:82–85. https://doi.org/10.1002/dc.2840090118.

18. Chetty A. 2003. Pathology of allergic bronchopulmonary aspergillosis. Front Biosci 8:e110–e114. https://doi.org/10.2741/945.

19. Kowalski CH, Beattie SR, Fuller KK, McGurk EA, Tang Y-W, Hohl TM, Obar JJ, Cramer RA, Jr. 2016. Heterogeneity among isolates reveals that fitness in low oxygen correlates with Aspergillus fumigatus virulence. mBio 7:e01515-16. https://doi.org/10.1128/mBio.01515-16.

20. Caffrey-Carr AK, Kowalski CH, Beattie SR, Blaseg NA, Upshaw CR, Thammahong A, Lust HE, Tang Y-W, Hohl TM, Cramer RA, Obar JJ. 2017. Interleukin 1α is critical for resistance against highly virulent Aspergillus fumigatus isolates. Infect Immun 85:e00661-17. https://doi.org/10.1128/IAI.00661-17.

21. Jhingran A, Mar KB, Kumasaka DK, Knoblaugh SE, Ngo LY, Segal BH, Iwakura Y, Lowell CA, Hamerman JA, Lin X, Hohl TM. 2012. Tracing conidial fate and measuring host cell antifungal activity using a reporter of microbial viability in the lung. Cell Rep 2:1762–1773. https://doi.org/10.1016/j.celrep.2012.10.026.

22. Patel AR, Patel AR, Singh S, Singh S, Khawaja I. 2019. Diagnosing allergic bronchopulmonary aspergillosis: a review. Cureus 11:e4550. https://doi.org/10.7759/cureus.4550.

23. Fukahori S, Matsuse H, Tsuchida T, Kawano T, Nishino T, Fukushima C, Kohno S. 2014. Clearance of Aspergillus fumigatus is impaired in the airway in allergic inflammation. Ann Allergy Asthma Immunol 113:180–186. https://doi.org/10.1016/j.anai.2014.05.011.

24. Keown K, Abbott S, Kuzeljevic B, Rayment JH, Chilvers MA, Yang CL. 2019. An investigation into biomarkers for the diagnosis of ABPA and aspergillus disease in cystic fibrosis. Pediatr Pulmonol 54:1787–1793. https://doi.org/10.1002/ppul.24465.

25. Agarwal R, Chakrabarti A, Shah A, Gupta D, Meis JF, Guleria R, Moss R, Denning DW, ABPA complicating asthma ISHAM working group. 2013. Allergic bronchopulmonary aspergillosis: review of literature and proposal of new diagnostic and classification criteria. Clin Exp Allergy 43:850–873. https://doi.org/10.1111/cea.12141.

26. Shlezinger N, Irmer H, Dhingra S, Beattie SR, Cramer RA, Braus GH, Sharon A, Hohl TM. 2017. Sterilizing immunity in the lung relies on targeting fungal apoptosis-like programmed cell death. Science 357:1037–1041. https://doi.org/10.1126/science.aan0365.

27. Boyle KB, Stephens LR, Hawkins PT. 2012. Activation of the neutrophil NADPH oxidase by Aspergillus fumigatus. Ann N Y Acad Sci 1273:68–73. https://doi.org/10.1111/j.1749-6632.2012.06821.x.

28. Paris S, Wysong D, Debeaupuis JP, Shibuya K, Philippe B, Diamond RD, Latgé JP. 2003. Catalases of Aspergillus fumigatus. Infect Immun 71:3551–3562. https://doi.org/10.1128/iai.71.6.3551-3562.2003.

29. Calera JA, Paris S, Monod M, Hamilton AJ, Debeaupuis JP, Diaquin M, López-Medrano R, Leal F, Latgé JP. 1997. Cloning and disruption of the antigenic catalase gene of Aspergillus fumigatus. Infect Immun 65:4718–4724. https://doi.org/10.1128/IAI.65.11.4718-4724.1997.

30. Lessing F, Kniemeyer O, Wozniok I, Loeffler J, Kurzai O, Haertl A, Brakhage AA. 2007. The Aspergillus fumigatus transcriptional regulator AfYap1 represents the major regulator for defense against reactive oxygen intermediates but is dispensable for pathogenicity in an intranasal mouse infection model. Eukaryot Cell 6:2290–2302. https://doi.org/10.1128/EC.00267-07.

31. Milroy CM, Blanshard JD, Lucas S, Michaels L. 1989. Aspergillosis of the nose and paranasal sinuses. J Clin Pathol 42:123–127. https://doi.org/10.1136/jcp.42.2.123.

32. Pokharel S, Ylagan L, Cheney R. 2014. Allergic bronchopulmonary aspergillosis: a diagnostic challenge. J Cytol Histol S4:2. https://doi.org/10.4172/2157-7099.S4-021.

33. Akoumianaki T, Kyrmizi I, Valsecchi I, Gresnigt MS, Samonis G, Drakos E, Boumpas D, Muszkieta L, Prevost MC, Kontoyiannis DP, Chavakis T, Netea MG, Van De Veerdonk FL, Brakhage AA, El-Benna J, Beauvais A, Latge JP, Chamilos G. 2016. Aspergillus cell wall melanin blocks LC3-associated phagocytosis to promote pathogenicity. Cell Host Microbe 19:79–90. https://doi.org/10.1016/j.chom.2015.12.002.

34. Ramaprakash H, Shibata T, Duffy KE, Ismailoglu UB, Bredernitz RM, Moreira AP, Coelho AL, Das AM, Fursov N, Chupp GL, Hogaboam CM. 2011. Targeting ST2L potentiates CpG-mediated therapeutic effects in a chronic fungal asthma model. Am J Pathol 179:104–115. https://doi.org/10.1016/j.ajpath.2011.03.032.

35. Schuh JM, Blease K, Hogaboam CM. 2002. CXCR2 is necessary for the development and persistence of chronic fungal asthma in mice. J Immunol 168:1447–1456. https://doi.org/10.4049/jimmunol.168.3.1447.

36. Su Y-C, Rolph MS, Hansbro NG, Mackay CR, Sewell WA. 2008. Granulocyte-macrophage colony-stimulating factor is required for bronchial eosinophilia in a murine model of allergic airway inflammation. J Immunol 180:2600–2607. https://doi.org/10.4049/jimmunol.180.4.2600.

37. Bonecchi R, Bianchi G, Bordignon PP, D'Ambrosio D, Lang R, Borsatti A, Sozzani S, Allavena P, Gray PA, Mantovani A, Sinigaglia F. 1998. Differential expression of chemokine receptors and chemotactic responsiveness of type 1 T helper cells (Th1s) and Th2s. J Exp Med 187:129–134. https://doi.org/10.1084/jem.187.1.129.

38. Gauthier M, Chakraborty K, Oriss TB, Raundhal M, Das S, Chen J, Huff R, Sinha A, Fajt M, Ray P, Wenzel SE, Ray A. 2017. Severe asthma in humans and mouse model suggests a CXCL10 signature underlies corticosteroid-resistant Th1 bias. JCI Insight 2:e94580. https://doi.org/10.1172/jci.insight.94580.

39. Hogaboam CM, Blease K, Mehrad B, Steinhauser ML, Standiford TJ, Kunkel SL, Lukacs NW. 2000. Animal model: chronic airway hyperreactivity, goblet cell hyperplasia, and peribronchial fibrosis during allergic airway disease induced by Aspergillus fumigatus. Am J Pathol 156:723–732. https://doi.org/10.1016/S0002-9440(10)64775-X.

40. Allard JB, Poynter ME, Marr KA, Cohn L, Rincon M, Whittaker LA. 2006. Aspergillus fumigatus generates an enhanced Th2-biased immune response in mice with defective cystic fibrosis transmembrane conductance regulator. J Immunol 177:5186–5194. https://doi.org/10.4049/jimmunol.177.8.5186.

41. Chaudhary N, Datta K, Askin FB, Staab JF, Marr KA. 2012. Cystic fibrosis transmembrane conductance regulator regulates epithelial cell response to Aspergillus and resultant pulmonary inflammation. Am J Respir Crit Care Med 185:301–310. https://doi.org/10.1164/rccm.201106-1027OC.

42. Iannitti RG, Napolioni V, Oikonomou V, De Luca A, Galosi C, Pariano M, Massi-Benedetti C, Borghi M, Puccetti M, Lucidi V, Colombo C, Fiscarelli E, Lass-Flörl C, Majo F, Cariani L, Russo M, Porcaro L, Ricciotti G, Ellemunter H, Ratclif L, De Benedictis FM, Talesa VN, Dinarello CA, van de Veerdonk FL, Romani L. 2016. IL-1 receptor antagonist ameliorates inflammasome-dependent inflammation in murine and human cystic fibrosis. Nat Commun 7:10791. https://doi.org/10.1038/ncomms10791.

43. National Research Council. 2011. Guide for the care and use of laboratory animals, 8th ed. National Academies Press, Washington, DC.

44. Grahl N, Puttikamonkul S, Macdonald JM, Gamcsik MP, Ngo LY, Hohl TM, Cramer RA. 2011. In vivo hypoxia and a fungal alcohol dehydrogenase

influence the pathogenesis of invasive pulmonary aspergillosis. PLoS Pathog 7:e1002145. https://doi.org/10.1371/journal.ppat.1002145.

45. Kowalski CH, Kerkaert JD, Liu K-W, Bond MC, Hartmann R, Nadell CD, Stajich JE, Cramer RA. 2019. Fungal biofilm morphology impacts hypoxia fitness and disease progression. Nat Microbiol 4:2430–2412. https://doi.org/10.1038/s41564-019-0558-7.

46. Huang DW, Sherman BT, Lempicki RA. 2009. Bioinformatics enrichment tools: paths toward the comprehensive functional analysis of large gene lists. Nucleic Acids Res 37:1–13. https://doi.org/10.1093/nar/gkn923.

47. Huang DW, Sherman BT, Tan Q, Kir J, Liu D, Bryant D, Guo Y, Stephens R, Baseler MW, Lane HC, Lempicki RA. 2007. DAVID Bioinformatics Resources: expanded annotation database and novel algorithms to better extract biology from large gene lists. Nucleic Acids Res 35(Web Server issue):W169–W175. https://doi.org/10.1093/nar/gkm415.

48. Alexa A, Rahnenführer J, Lengauer T. 2006. Improved scoring of functional groups from gene expression data by decorrelating GO graph structure. Bioinformatics 22:1600–1607. https://doi.org/10.1093/bioinformatics/btl140.

49. Gu Z, Eils R, Schlesner M. 2016. Complex heatmaps reveal patterns and correlations in multidimensional genomic data. Bioinformatics 32:2847–2849. https://doi.org/10.1093/bioinformatics/btw313.

50. Griffiths LJ, Anyim M, Doffman SR, Wilks M, Millar MR, Agrawal SG. 2006. Comparison of DNA extraction methods for Aspergillus fumigatus using real-time PCR. J Med Microbiol 55:1187–1191. https://doi.org/10.1099/jmm.0.46510-0.

51. Stajich JE, Harris T, Brunk BP, Brestelli J, Fischer S, Harb OS, Kissinger JC, Li W, Nayak V, Pinney DF, Stoeckert CJ, Roos DS. 2012. FungiDB: an integrated functional genomics database for fungi. Nucleic Acids Res 40(Database issue):D675–D681. https://doi.org/10.1093/nar/gkr918.

52. Basenko EY, Pulman JA, Shanmugasundram A, Harb OS, Crouch K, Starns D, Warrenfeltz S, Aurrecoechea C, Stoeckert CJ, Kissinger JC, Roos DS, Hertz-Fowler C. 2018. FungiDB: an integrated bioinformatic resource for fungi and oomycetes. J Fungi 4:39. https://doi.org/10.3390/jof4010039.

53. Li H, Wren J. 2014. Toward better understanding of artifacts in variant calling from high-coverage samples. Bioinformatics 30:2843–2851. https://doi.org/10.1093/bioinformatics/btu356.

54. Li H, Handsaker B, Wysoker A, Fennell T, Ruan J, Homer N, Marth G, Abecasis G, Durbin R, 1000 Genome Project Data Processing Subgroup. 2009. The Sequence Alignment/Map format and SAMtools. Bioinformatics 25:2078–2079. https://doi.org/10.1093/bioinformatics/btp352.

55. Van der Auwera GA, Carneiro MO, Hartl C, Poplin R, Del Angel G, Levy-Moonshine A, Jordan T, Shakir K, Roazen D, Thibault J, Banks E, Garimella KV, Altshuler D, Gabriel S, DePristo MA. 2013. From FastQ data to high confidence variant calls: the Genome Analysis Toolkit best practices pipeline. Curr Protoc Bioinformatics 43:11.10.1–11.10.33. https://doi.org/10.1002/0471250953.bi1110s43.

56. Cingolani P, Platts A, Wang LL, Coon M, Nguyen T, Wang L, Land SJ, Lu X, Ruden DM. 2012. A program for annotating and predicting the effects of single nucleotide polymorphisms, SnpEff: SNPs in the genome of Drosophila melanogaster strain w1118; iso-2; iso-3. Fly (Austin) 6:80–92. https://doi.org/10.4161/fly.19695.

57. Quinlan AR, Hall IM. 2010. BEDTools: a flexible suite of utilities for comparing genomic features. Bioinformatics 26:841–842. https://doi.org/10.1093/bioinformatics/btq033.

58. R Development Core Team. 2013. R: a language and environment for statistical computing. R Foundation for Statistical Computing, Vienna, Austria.

59. Stajich JE, Lofgren LA. 2020. stajichlab/W72310: W72310 variant pipeline. https://zenodo.org/record/4116457#.X8k75KpKgWo.